

calcium phosphate coprecipitation technique. After 48 hours, transfected cells were washed with medium containing 2 mM EDTA and then with culture medium. Cells were then challenged with HIV-1 LAI (corresponding to 0.5  $\mu$ g of p25, which is equivalent to about 40 particles per cell) for 6 hours in the absence or presence of inhibitors. Cells were first washed in medium containing 2 mM EDTA and then washed once with trypsin before incubation (5 min at 37°C) in 5 ml of trypsin. Cells were then replated in 75-cm<sup>2</sup> flasks containing fresh culture medium and incubated at 37°C for 24 hours. One-milliliter portions of each supernatant were then used to infect CEM cells ( $5 \times 10^6$ ). The production of HIV-1 (as determined by ELISA of p25) in CEM cultures was measured by assaying culture supernatants 7, 9, and 11 days later. The expression of CD4 antigen on the cell surface of transfected cells was carried out 48 hours after trypsin treatment by FACS analysis with mAb OKT4. [P. R. Rao, M. A. Talle, P. C. Kung, G. Goldstein, *Cell Immunol.* **80**, 310 (1983)]. The expression of human CD26 was determined

after immunoprecipitation (see Fig. 4, legend).  
 33. Supported by grants from Institut Pasteur, Paris, and Agence Nationale de la Recherche sur le SIDA. C.C. and E.J. were supported by Association des Artistes contre le SIDA. We thank I. Marié and N. Robert for assistance; A. Laurent-Crawford, M. A. Rey-Cuillé, and D. Cointe for discussion during this work; and B. Bauvois for advice on the assay of DPP IV activity and critical reading of the manuscript. Monoclonal antibody IF7 was kindly provided by C. Morimoto, Dana-Farber Cancer Institute, Harvard Medical School, Boston. The pLXSN-CD4 plasmid was obtained from O. Schwartz, Institut Pasteur, Paris. Plasmid pKG5 expressing human CD26 was kindly provided by B. Fleischer, Universität Mainz. Additional thanks go to R. Siraganian and B. R. G. Williams for critical reading of the manuscript. Special acknowledgments are forwarded to L. Montagnier for advice and continual support during the realization of this work.

1 October 1993; accepted 18 November 1993

in cell cycle progression, we examined the phenotypic consequences of the inactivation of each kinase. We generated dominant-negative mutations for each Cdc2-related kinase and expressed these mutant forms in human cells. When expressed at high levels, dominant-negative mutations inactivate the function of the wild-type protein by competing for essential interacting molecules (14). Data from previous structure-function studies predicted that the mutation of Asp<sup>145</sup> in Cdk2 (Asp<sup>146</sup> in Cdc2) might generate dominant-negative mutants. This residue is conserved in all protein kinases and is part of an amino acid stretch, KLAD\*FGLAR (11) (\* marks point of mutation), that is identical in all Cdc2-related genes (7, 15). The equivalent Asp residue in 3',5'-adenosine monophosphate (cAMP)-dependent kinase is known to be essential in the phospho-transfer reaction (16). On the basis of the crystal structure data, this residue presumably chelates Mg<sup>2+</sup> and orients the  $\beta$ - and  $\gamma$ -phosphates of magnesium adenosine triphosphate (Mg<sup>2+</sup>ATP) in the catalytic cleft of the enzyme (17). Moreover, an Asp to Asn point mutation at this position has been identified in one of the two dominant-negative mutant alleles that have been found for CDC28 in yeast (18). Finally, this residue is located outside the regions of *cdc2* that are implicated in binding cyclin and p13<sup>suc1</sup> subunits (19).

To determine whether dominant-negative inhibition could lead to specific loss of function, we tested the effects of the Asp to Asn mutation in Cdc2 and Cdk2. For each kinase, four versions were generated: wild type (wt) and mutant, each untagged or modified with an influenza hemagglutinin (HA) epitope tag at the COOH-terminus to allow discrimination between endogenous and exogenous kinases (20). When expressed from the inducible GAL4 promoter in yeast, wild-type tagged and untagged forms of Cdc2 and Cdk2 were able to rescue the *cdc28-4* allele at the nonpermissive temperature (36°C), indicating that the tagged kinases were functional (21). The corresponding mutant forms could not rescue *cdc28* mutations at the nonpermissive temperature. Moreover, these mutants interfered with proliferation when induced at the permissive temperature (21).

The wild-type and mutant kinases were cloned under the control of the cytomegalovirus (CMV) promoter and were transiently transfected into human U2OS osteosarcoma cells (20, 22). The expression levels of the wild-type and mutant proteins were similar (Fig. 1, B and C). However, *in vitro* histone H1 kinase activity was only associated with the wild-type kinases (Fig. 1D). The epitope-tagged forms of both wild-type and mutant Cdc2 appeared to associate with

## Distinct Roles for Cyclin-Dependent Kinases in Cell Cycle Control

Sander van den Heuvel\* and Ed Harlow

The key cell-cycle regulator Cdc2 belongs to a family of cyclin-dependent kinases in higher eukaryotes. Dominant-negative mutations were used to address the requirement for kinases of this family in progression through the human cell cycle. A dominant-negative Cdc2 mutant arrested cells at the G<sub>2</sub> to M phase transition, whereas mutants of the cyclin-dependent kinases Cdk2 and Cdk3 caused a G<sub>1</sub> block. The mutant phenotypes were specifically rescued by the corresponding wild-type kinases. These data reveal that Cdk3, in addition to Cdc2 and Cdk2, executes a distinct and essential function in the mammalian cell cycle.

Cell division is controlled by way of a complex network of biochemical signals that are similar in all eukaryotic cells. Together, these signals regulate specific transitions in the cell cycle. The best characterized transitions are those from G<sub>1</sub> to S phase and from G<sub>2</sub> to mitosis. In yeast, passage through both transition points is regulated by the same protein kinase, the product of the *CDC28* or *cdc2*<sup>+</sup> gene for *Saccharomyces cerevisiae* and *Schizosaccharomyces pombe*, respectively (1). The Cdc2-CDC28 catalytic subunit requires association with a cyclin regulatory subunit for kinase activity (2), and different cyclins are involved in the G<sub>1</sub>/S transition (G<sub>1</sub> cyclins) and the G<sub>2</sub>/M transition (mitotic cyclins). Multicellular eukaryotes appear to have developed a higher degree of regulation. They express multiple cyclins, like yeast, but also contain multiple catalytic subunits that can interact with these cyclins. Whereas p34<sup>cdc2</sup> is active and essential at the G<sub>2</sub>/M transition (3, 4), a closely related kinase, p33<sup>cdk2</sup>, has been implicated in

the initiation of DNA replication (3, 5, 6).

Twelve human protein kinases have been described that share extensive amino acid sequence identity with p34<sup>cdc2</sup> (7-10). These kinases are named temporarily after their amino acid sequence in the PSTAIRE-region (11), a domain that is conserved between yeast and human Cdc2. Alternatively, they are designated as cyclin-dependent kinases either when a cyclin partner is identified or when they complement yeast *cdc2-cdc28* mutations. In mammalian cells, Cdc2 associates mainly with A- and B-type cyclins; Cdk2 associates with cyclins A, E, and D; and Cdk4 (formerly PSK-J3), Cdk5 (previously PSSALRE), and Cdk6 (previously PLSTIRE) associate with D-type cyclins (5, 8, 10, 12, 13). Although Cdk3 has never been found in association with cyclins, because of high sequence identity with both Cdc2 and Cdk2 and the ability to complement *cdc28* mutations in yeast, it is classified as a cyclin-dependent kinase (7).

The existence of a family of Cdc2-related genes suggests that other kinases, in addition to Cdc2 and Cdk2, may regulate distinct steps in the cell cycle. To investigate the requirement for the other kinases

Massachusetts General Hospital Cancer Center, Charlestown, MA 02129.

\*To whom correspondence should be addressed.

cyclins A and B1, like endogenous Cdc2. The equivalent forms of Cdk2 bound to cyclins E and A (23). Thus, the Asp to Asn mutation in Cdc2 and Cdk2 abolished their function as kinases but did not affect their ability to associate with cyclins.

If wild-type Cdk2 and Cdc2 are required at specific times in the cell cycle, overexpression of dominant-negative mutants should block cell cycle progression when their kinase activity is required. We evaluated such phenotypes in transient transfection assays by including an expression plasmid for the B cell surface marker CD20. Transfected cells were identified by CD20 staining, and the cell cycle profile of the CD20-positive cells was determined by flow cytometry (22). Within the same experiment, the G<sub>1</sub>, S, and G<sub>2</sub>/M populations varied by a few percent at most between samples that were independently transfected with the same plasmids. Four different human cell lines with high transfection efficiencies were used in these experiments: U2OS and Saos-2 osteosarcoma cells, C33A cervical carcinoma cells, and T98G glioblastoma cells.

Expression of mutant Cdk2 and mutant Cdc2 changed the cell cycle distribution. The Cdk2 mutant (Cdk2-dn) caused a large increase in the G<sub>1</sub> population, whereas the Cdc2 mutant (Cdc2-dn) led to an increased G<sub>2</sub>/M population (Fig. 1A). Transfection of wild-type Cdc2 or Cdk2 did not affect the cell cycle distribution (24). However, the effect of the mutant kinase could be overcome in each case by the cotransfection of a plasmid expressing the corresponding wild-type kinase (Fig. 1A). Whereas the Cdk2-dn caused an effect in all cell lines tested, a Cdc2-dn effect was not observed in C33A cells (25).

Together, these data suggest that the arrests observed after the overexpression of mutant Cdk2 or Cdc2 are the result of specific inhibition of the activity of the endogenous wild-type kinases. The timing of the arrest is distinct for the Cdc2 and Cdk2 mutants and is consistent with the timing of activation of the endogenous kinases, as well as their predicted roles in cell cycle progression (3–6). It is unlikely that the effects are the result of nonspecific toxic effects because plasmids expressing the wild-type kinases gave no such change and could overcome the phenotype of the corresponding mutant. Therefore, we conclude that these mutants act in a dominant-negative fashion and create highly specific loss-of-function phenotypes.

If the effects of Cdk2 and Cdc2 mutants were the result of competition with the endogenous wild-type kinases for cyclin binding, the block should be overcome by overexpression of cyclins. Plasmids expressing cyclins A, B1, B2, C, D1, D3, and E

were transfected to test this possibility (26). Rescue of the Cdk2 dominant-negative effect was observed when a reduced amount of the mutant, resulting in a less stringent arrest, was transfected in a 1:2 ratio with the cyclin D1 plasmid (Fig. 2). Cyclins A and E were both less efficient in rescuing the inhibition, but their effectiveness was proportional to the level of their expres-

sion. No effects were observed when cyclins B1, B2, C, and D3 were cotransfected with the Cdk2 mutant. In contrast, a reduction of the Cdc2 dominant-negative effect was only observed when either cyclin B1 or B2 was coexpressed (27).

Although the rescue of Cdk2 and Cdc2 mutants by different cyclins points to specificity for G<sub>1</sub> versus mitotic cyclins, the

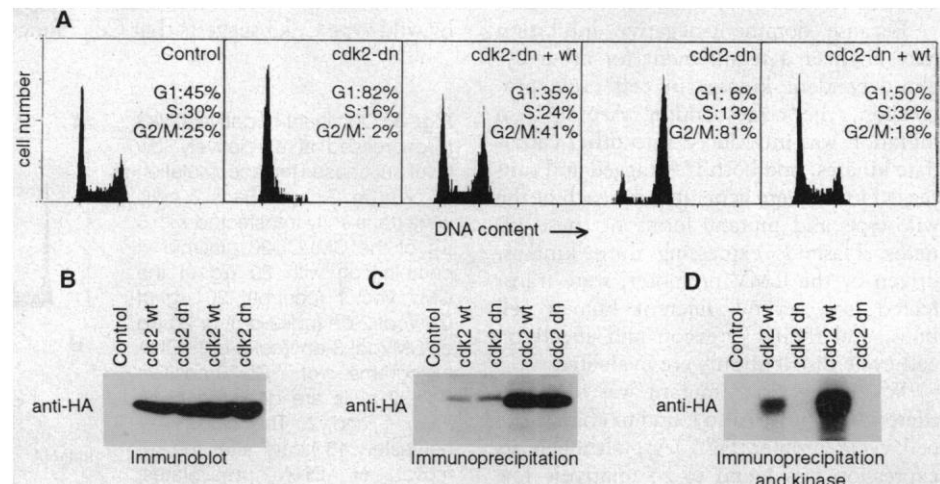
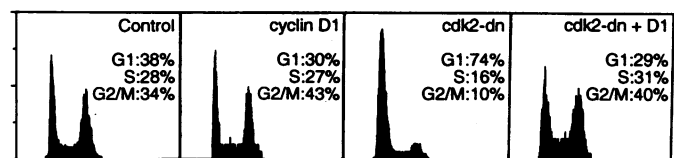


**Fig. 1.** Expression of mutant forms of Cdk2 and Cdc2 cause specific cell-cycle arrests. U2OS cells were transiently transfected with plasmids expressing the kinases indicated. Control cells are transfected with the CMV-neo-Bam vector. Dominant-negative (dn) and wild-type (wt) kinases were untagged in (A) whereas HA-tagged forms were expressed in (B), (C), and (D). (A) DNA histograms of CD20-positive cell populations in which relative DNA content is plotted against cell number. U2OS cells were transfected with 5  $\mu$ g of pCMVCD20 plus 20  $\mu$ g of CMV vector (control), 10  $\mu$ g of CMVcdk2-dn and 10  $\mu$ g of CMV vector (cdk2-dn), 10  $\mu$ g of CMVcdk2-dn and 10  $\mu$ g of CMVcdk2-wt (cdk2-dn + wt), 10  $\mu$ g of CMVcdc2-dn and 10  $\mu$ g of CMV vector (cdc2-dn), or 10  $\mu$ g of CMVcdc2-dn and 10  $\mu$ g of CMVcdc2-wt (cdc2-dn + wt). The cells were harvested 48 hours after the removal of DNA precipitates, stained for CD20 expression and DNA content, and analyzed by flow cytometry (33). (B) Expression levels of epitope-tagged mutant and wild-type Cdk2 and Cdc2 as determined by protein immunoblotting. Each lane contains 25  $\mu$ g of total lysate from cells transfected with 20  $\mu$ g of the CMV-neo-Bam vector (control) or 20  $\mu$ g of CMV plasmids expressing the indicated genes. Proteins were separated by SDS-PAGE (polyacrylamide gel electrophoresis), immunoblotted, and probed with the anti-HA monoclonal antibody 12CA5 as described (33). Similar results have been obtained with U2OS and C33A cells. To be able to compare expression levels of the different kinases, we used the same experiment and exposure for Fig. 3, B through D, and Fig. 4. (C) Immunoprecipitation of epitope-tagged mutant and wild-type Cdk2 and Cdc2. The anti-HA tag monoclonal antibody 12CA5 was used to immunoprecipitate <sup>35</sup>S-labeled proteins from U2OS cells transfected with the indicated plasmids. Medium was replaced 42 hours after transfection by 3 ml of methionine-free DMEM supplemented with 0.5-mCi <sup>35</sup>S-protein labeling mix (NEN) per dish. The cells were lysed in E1A-lysis buffer, and 1/10 of each lysate was immunoprecipitated with 12CA5 and protein A beads as described (33). (D) In vitro histone H1 kinase activity associated with anti-HA immunoprecipitates. Transfections and immunoprecipitations were performed as in (C), but 200  $\mu$ g of total cellular protein was used for each immunoprecipitation, followed by incubation of the immunoprecipitates in kinase buffer supplemented with 4  $\mu$ g of histone H1 and 40- $\mu$ M [<sup>32</sup>P]ATP at 30°C for 30 min as described (8).

**Fig. 2.** Rescue of the Cdk2 dominant-negative phenotype by overexpression of cyclin D1. Saos-2 cells were transiently transfected with 2  $\mu$ g of the CMVCD20 plasmid in combination with 24  $\mu$ g of the CMV vector (control), 16  $\mu$ g of cyclin D1 plasmid and 8  $\mu$ g of the vector (D1), 8  $\mu$ g of CMVcdk2-dn and 16  $\mu$ g of vector (cdk2-dn), or 8  $\mu$ g of CMVcdk2-dn and 16  $\mu$ g of cyclin D1 plasmid. DNA histograms of CD20-positive Saos-2 cells are shown in which DNA content is plotted versus cell number as in Fig. 1. Cells were harvested 48 hours after the removal of DNA precipitates, stained, and analyzed by flow cytometry as in Fig. 1 and (22).



effect was highly dependent on the relative amount of the rescuing cyclin. Therefore, whereas the alleviation of the dominant-negative effects suggests that cyclin titration is at least part of the mechanism of inhibition, it does not necessarily reveal the cyclins that regulate the kinase *in vivo*. This restriction is substantiated by our inability to detect endogenous cyclin D1 in Saos-2 cells, although the Cdk2-dn effect could be rescued by cyclin D1 in these cells.

Because dominant-negative inhibition may uncover a requirement for other cyclin-dependent kinases in cell cycle progression, the corresponding Asp mutation was introduced into other candidate kinases, and both HA-tagged and -untagged forms were generated for each of the wild-type and mutant forms of these kinases. Plasmids expressing these kinases, driven by the CMV promoter, were transfected into several different human cell lines, and their expression and effects on cell cycle distribution were evaluated.

When the Cdk3 mutant was tested in these assays, it was also found to change the cell cycle profile (Fig. 3A), although its expression was found to be relatively low (Fig. 3D). The Cdk3 mutant resulted in an increased G<sub>1</sub> population in all 15 independent experiments in Saos-2 and C33A cells (mean  $\pm$  SD, 24.2%  $\pm$  10.6%). Transfection of plasmids expressing wild-type Cdk3 did not have any noticeable effect.

We have supposed above that alteration of the flow cytometry profile by the dominant-negative mutants results from a block in cell cycle progression. However, another possibility is, in the case of Cdk3, that the mutant causes a G<sub>1</sub> increase as the consequence of the acceleration of S or G<sub>2</sub>/M. To discriminate between these possibilities, we examined the effect of nocodazole on the Cdk3 dominant-negative phenotype. Nocodazole, which prevents spindle formation, causes cells that proceed through the cycle to accumulate in M phase. However, this drug should have no effect if the cells are already arrested in G<sub>1</sub>. A substantial increase in the S and G<sub>2</sub>/M populations was observed in control transfected cells when nocodazole was added 48 hours after transfection and cells were harvested 16 hours later. However, cells expressing the Cdk3-dn mutant did not accumulate in G<sub>2</sub>/M (Fig. 3E). The lack of a nocodazole effect was specific for the Cdk3-dn- and CD20-positive cells because the same sample showed a large enrichment of cells at G<sub>2</sub>/M when untransfected cells were included (Fig. 3E). Thus, the Cdk3 mutant causes a G<sub>1</sub> arrest and not acceleration of S or G<sub>2</sub>/M.

Rescue experiments were performed to test the specificity of dominant-negative Cdk2 and Cdk3 because both mutants caused the accumulation of cells in G<sub>1</sub>. The

amount of mutant plasmid was reduced to lower the dominant-negative effect and make rescue as sensitive as possible. Whereas wild-type Cdk2 could efficiently overcome the dominant-negative effect of the Cdk2 mutant, wild-type Cdk3 could not (Table 1). In the converse experiment, wild-type Cdk3 neutralized the effect of the Cdk3 mutant, but wild-type Cdk2 did not (Table 1). The fact that dominant-negative Cdk3 causes a G<sub>1</sub> block that can be rescued by wild-type Cdk3 suggests that Cdk3 func-

tion is required for G<sub>1</sub> progression.

The same increase in the G<sub>1</sub> population could be obtained with amounts of the Cdk3 mutant 1/10 to 1/20 that of the Cdk2 mutant (28). Because a relatively low amount of the Cdk3 mutant caused a dominant-negative phenotype, the endogenous amount of this kinase might be low. An affinity-purified rabbit antiserum raised against the 10 amino acids of the COOH-terminus of Cdk3 readily detected 36- and 33-kD proteins from Cdk3-transfected cells

**Fig. 3.** Dominant-negative Cdk3 is expressed at a relatively low level but causes the accumulation of cells in G<sub>1</sub>. (A) Saos-2 cells were transiently transfected with 5  $\mu$ g of the CMVCD20 plasmid in combination with 20  $\mu$ g of the CMV vector (control), 20  $\mu$ g of CMVcdk2-dn (cdk2-dn), or 20  $\mu$ g of CMVcdk3-dn (cdk3-dn). DNA histograms of CD20-positive Saos-2 cells are depicted as in Figs. 1 and 2. The cells were harvested 48 hours after the removal of DNA precipitates, stained, and analyzed by flow cytometry (22). The expression levels of epitope-tagged mutant and wild-type Cdk2 and Cdk3 were determined by protein immunoblotting. Arrows indicate the position of Cdk2 and Cdk3 proteins. Each lane contains 25  $\mu$ g of total lysate from cells transfected with (B) 20  $\mu$ g of the CMV-neo-Bam vector (control), (C) 20  $\mu$ g of CMVcdk2-dn, or (D) 20  $\mu$ g of Cdk3-dn. Proteins were separated by SDS-PAGE, immunoblotted, and probed with the HA monoclonal antibody 12CA5. To compare expression levels of the different kinases, the same experiment and exposure is used for each panel, as in Fig. 1B and Fig. 4. (E) Cells expressing Cdk3-dn are blocked in G<sub>1</sub>. Forty-eight hours after transfection, cells were refed with fresh medium (upper panel) or fresh medium containing nocodazole (NOC) (50 ng/ml; lower panel). The cells were harvested, stained, and analyzed by flow cytometry 16 hours later. Saos-2 cells were transfected with 3  $\mu$ g of CMVCD20 in combination with (left) 22  $\mu$ g of CMV vector or (middle and right) 22  $\mu$ g of CMVcdk3-dn. Left and middle histograms show the DNA content of the CD20-positive populations. Histograms at the right show the total population and include  $\geq$ 90% untransfected cells. The middle and right histograms are derived from the same samples.

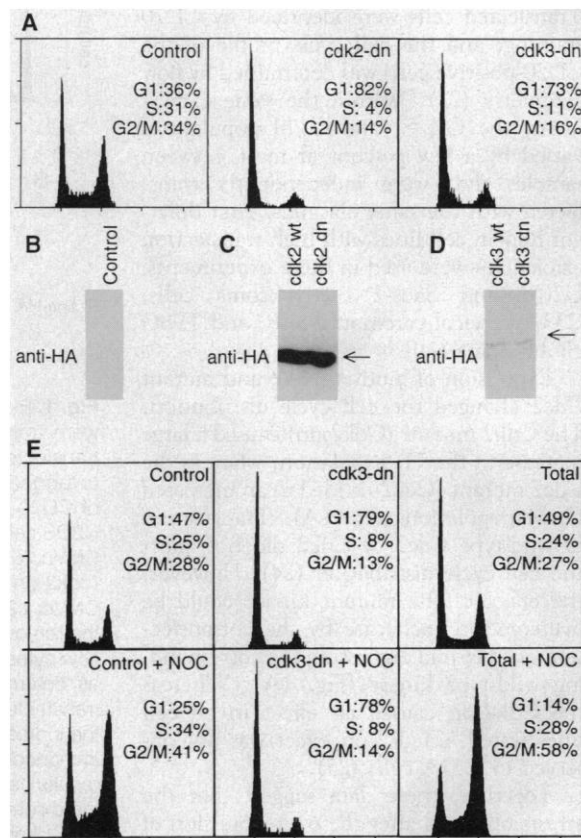


**Table 1.** Rescue of the Cdk2 and Cdk3 dominant-negative phenotype by coexpression of the corresponding wild-type kinases. Saos-2 cells were transiently transfected with 2  $\mu$ g of the CMVCD20 vector in combination with either 20  $\mu$ g of vector DNA or 10  $\mu$ g of each plasmid indicated below. The cell cycle profile of CD20-positive cells (percentage of cells in each stage) was determined by flow cytometry (22). Each value is the mean  $\pm$  SD of four independent experiments.

	Vector	Cdk2-dn + vector	Cdk2-dn + Cdk2-wt	Cdk2-dn + Cdk3-wt	Cdk3-dn + vector	Cdk3-dn + Cdk3-wt	Cdk3-dn + Cdk2-wt
G <sub>1</sub>	43 $\pm$ 4	79 $\pm$ 5	38 $\pm$ 11	77 $\pm$ 5	66 $\pm$ 12	45 $\pm$ 7	55 $\pm$ 9
S	33 $\pm$ 4	14 $\pm$ 6	27 $\pm$ 3	15 $\pm$ 4	20 $\pm$ 8	26 $\pm$ 1	21 $\pm$ 2
G <sub>2</sub> /M	24 $\pm$ 1	7 $\pm$ 3	35 $\pm$ 11	8 $\pm$ 3	14 $\pm$ 4	29 $\pm$ 6	24 $\pm$ 7

and proteins with the same mobility at much lower levels in untransfected normal human fibroblasts (WI38) and human tumor cell lines (29). The expression of the Cdk3 proteins was roughly two orders of magnitude lower than that of Cdk2, as determined from the signal obtained when Cdk2 and Cdk3 immunoprecipitations were immunoblotted and probed with an anti-PSTAIRES monoclonal antibody. To date, we have been unable to detect cyclins associated with Cdk3 in experiments in which Cdk2- and Cdc2-associated cyclins were readily detected. However, cotransfection with cyclins D1 or E could largely overcome the dominant-negative Cdk3 effect, which is an indication that Cdk3 requires a cyclin partner for its function (27).

Transfection of plasmids encoding wild-type or mutant forms of Cdk4, Cdk5, Cdk6, and PCTAIRES-1 had no noticeable effect on the cell cycle distribution of transfected C33A, Saos-2, U2OS, or T98G cells (Fig. 4). Moderate (Cdk6) to very high levels of each kinase were found in transfected cells (Fig. 4). In several cases, we tested for redundancy by cotransfection of related kinases. For example, Cdk4 and Cdk6 share 71% identity in amino acid sequence (7); however, cotransfection of the Cdk4 and

Cdk6 mutants did not affect cell cycle distribution. Neither did combinations involving three or four of these mutant kinases. In this assay system, we cannot identify an essential role for the Cdk4, Cdk5, Cdk6, or PCTAIRES-1 kinases in cell cycle progression, but experiments in other systems will be required to evaluate such functions. Kinase activity associated with Cdk5 has been detected solely in terminally differentiated neuronal cells, suggesting that its function is unrelated to cell division (30).

Data from this and other studies suggest that different catalytic subunits have evolved in higher eukaryotes to control distinct cell cycle events (3-6). In addition to Cdc2 and Cdk2, Cdk3 appears to be one of such catalytic subunits. The phenotype of the dominant-negative Cdk3 mutant suggests that cellular Cdk3 executes a G<sub>1</sub> regulatory function. Several observations support this conclusion: (i) The effects of dominant-negative cyclin-dependent kinases were highly specific. The phenotypes of mutant Cdc2 and Cdk2 are distinct and consistent with their presumed functions, and mutant forms of several closely related kinases did not have any cell cycle effect. (ii) Coexpression of wild-type Cdk3 efficiently reversed the effect of mutant Cdk3. (iii) Growth arrest by dominant-negative

Cdk3 occurred at relatively low expression levels, in agreement with the low amount of the endogenous protein. (iv) Overexpression of G<sub>1</sub> cyclins can overcome the effect of dominant-negative Cdk3. (v) In previous work, Cdk3 was shown to be the only kinase in addition to Cdk2 and Cdc2 that could rescue yeast *cdc28* mutations (7). Together, our data suggest that the Cdk2 and Cdk3 kinases play essential and independent roles in G<sub>1</sub>/S progression.

## REFERENCES AND NOTES

- L. H. Hartwell *et al.*, *Science* **183**, 46 (1974); P. Nurse and Y. Bissett, *Nature* **292**, 558 (1981); S. I. Reed and C. Wittenberg, *Proc. Natl. Acad. Sci. U.S.A.* **87**, 5697 (1990).
- G. Draetta, *Trends Biochem. Sci.* **15**, 378 (1990); S. L. Forsburg and P. Nurse, *Annu. Rev. Cell Biol.* **7**, 227 (1991); J. Pines and T. Hunter, *New Biol.* **2**, 389 (1990).
- F. Fang and J. W. Newport, *Cell* **66**, 731 (1991).
- J. P. Th'ng *et al.*, *ibid.* **63**, 313 (1990); K. Riabowol *et al.*, *ibid.* **57**, 393 (1989).
- L.-H. Tsai, E. Lees, B. Faha, E. Harlow, K. Riabowol, *Oncogene* **8**, 1593 (1993).
- M. Pagano *et al.*, *J. Cell Biol.* **121**, 101 (1993).
- M. Meyerson *et al.*, *EMBO J.* **11**, 2909 (1992).
- L.-H. Tsai *et al.*, *Nature* **353**, 174 (1991).
- S. K. Hanks, *Proc. Natl. Acad. Sci. U.S.A.* **84**, 388 (1987); J. Ninomiya-Tsuji, S. Nomoto, H. Yasuda, S. I. Reed, K. Matsumoto, *ibid.* **88**, 9006 (1991); S. J. Elledge and M. R. Spottswood, *EMBO J.* **10**, 2653 (1991); Y. Lapidot-Lifson *et al.*, *Proc. Natl. Acad. Sci. U.S.A.* **89**, 579 (1992).
- Y. Xiong, H. Zhang, D. Beach, *Cell* **71**, 505 (1992).
- Abbreviations for the amino acid residues: A, Ala; C, Cys; D, Asp; E, Glu; F, Phe; G, Gly; H, His; I, Ile; K, Lys; L, Leu; M, Met; N, Asn; P, Pro; Q, Gln; R, Arg; S, Ser; T, Thr; V, Val; W, Trp; and Y, Tyr.
- J. Pines and T. Hunter, *Nature* **346**, 760 (1990); G. Draetta and D. Beach, *Cell* **54**, 17 (1988); J. Pines and T. Hunter, *ibid.* **58**, 833 (1989); J. Rosenblatt, Y. Gu, D. O. Morgan, *Proc. Natl. Acad. Sci. U.S.A.* **89**, 2824 (1992); A. Koff *et al.*, *Science* **257**, 1689 (1992); E. Lees, B. Faha, V. Dulić, S. I. Reed, E. Harlow, *Genes Dev.* **6**, 1874 (1992); V. Dulić, E. Lees, S. I. Reed, *Science* **257**, 1958 (1992); H. Matsushime *et al.*, *Cell* **71**, 323 (1992).
- M. Meyerson and E. Harlow, *Mol. Cell Biol.*, in press.
- I. Herskowitz, *Nature* **329**, 219 (1987).
- S. K. Hanks, A. M. Quinn, T. Hunter, *Science* **241**, 42 (1988).
- S. S. Taylor *et al.*, *Trends Biochem. Sci.* **18**, 84 (1993).
- D. R. Knighton *et al.*, *Science* **253**, 407 (1991); D. R. Knighton *et al.*, *ibid.*, p. 414; H. L. DeBont *et al.*, *Nature* **363**, 595 (1993).
- M. D. Mendenhall, H. E. Richardson, S. I. Reed, *Proc. Natl. Acad. Sci. U.S.A.* **85**, 4426 (1988).
- B. Ducommun, P. Brambilla, G. Draetta, *Mol. Cell Biol.* **11**, 6177 (1991); B. Ducommun *et al.*, *EMBO J.* **10**, 3311 (1991).
- Point mutations were introduced by *in vitro* mutagenesis. The DNA clones containing the open reading frames for each kinase were inserted into the Bam HI site of the pSelect vector (Promega), denatured, annealed to two different primers, and used for DNA synthesis, ligation, and transformation. One primer that contained a single mismatch in the middle was specific for each kinase and overlapped with most of the KLADFLG (11) encoding sequence. The DNA clones containing mutations were identified by DNA sequencing after a second transformation. A 7-amino acid epitope tag (YDVPDYA) was inserted just before the stop codon of each kinase, either by *in vitro* mutagenesis or by polymerase chain reaction (PCR). DNA sequencing was used to confirm the sequence of the tag. The complete open reading frame of the clones generated

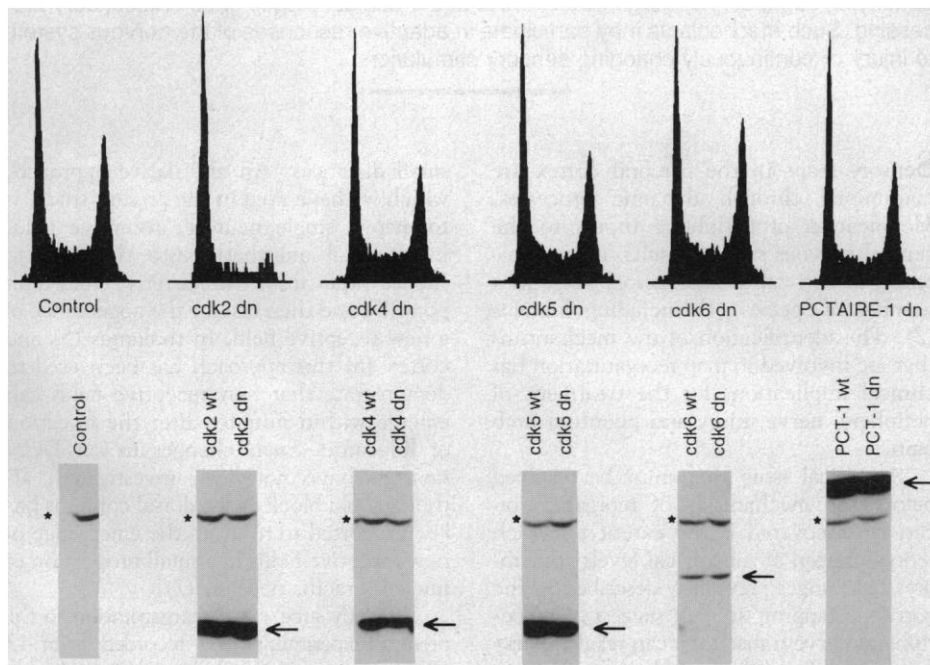


**Fig. 4.** Expression of mutant Cdk4, Cdk5, Cdk6, or PCTAIRES-1 (PCT-1) does not result in significant changes in cell cycle distribution. The top panel contains DNA histograms from CD20-positive C33A cells. DNA content is displayed versus cell number, as in Fig. 1. C33A cells were transiently transfected with 5  $\mu$ g of pCMVCD20 in combination with 20  $\mu$ g of plasmid DNA expressing the kinases indicated. The cells were harvested 48 hours after the removal of DNA precipitates, stained, and analyzed by flow cytometry (22). The lower panel shows the expression levels of epitope-tagged mutant and wild-type kinases as determined by protein immunoblotting. Arrows indicate the positions of each kinase. Asterisks indicate a cellular protein recognized by the 12CA5 antibody. Each lane contains 25  $\mu$ g of total lysate from transfected C33A cells. Proteins were separated by SDS-PAGE, immunoblotted, and probed with the anti-HA monoclonal antibody 12CA5. To compare expression levels of the different kinases, the same exposure was used for each panel, as in Figs. 1B and 3, B through D.

- by PCR was sequenced. The inserts were cloned into the Bam HI site of the CMV-neo-Bam vector (31) for expression in human cells.
21. For expression in *S. cerevisiae*, the coding regions of Cdc2 and Cdk2, mutant and wild-type and both tagged and untagged, were cloned into the Bam HI site of pMR438. The vector contains a *GAL1* promoter upstream of the inserted genes, a yeast 2 $\mu$  origin of replication, and a *URA3* selectable marker. All plasmids were tested in *S. cerevisiae* strain 10083-5C (*MATa GAL cdc28-4 gcn4 ura3*), and several were tested in K699 (*MATa GAL cdc28-1N ade-1-1 can1-100 his3-11 leu2 trp1-1 ura3*). Plasmids were transformed into yeast by the lithium acetate method and selected on plates lacking uracil and containing 2% glucose. Transformants were tested on plates containing either 2% glucose or 2% galactose at the permissive temperature (25°C) or nonpermissive temperature (36°C) as described (7).
  22. Cells were split 1:5 (Saos-2, C33A) or 1:8 (U2OS) and were transfected 20 hours later with calcium-phosphate precipitates of 20 to 26  $\mu$ g of plasmid DNA for each 100-mm dish (32). After 16 hours, the cells were washed twice with phosphate-buffered saline (PBS) and incubated with fresh medium [Dulbecco's minimum essential medium (DMEM) with 10% fetal bovine serum (FBS)]. Forty-eight hours after the removal of DNA precipitates, cells were rinsed off the plates with PBS containing 0.1% EDTA, pelleted, and stained with 20  $\mu$ l of a fluorescein isothiocyanate (FITC)-conjugated anti-CD20 monoclonal antibody, as described (33). Subsequently, cells were washed twice and fixed overnight in 80% ethanol. Before analysis, the cells were pelleted, washed once, and stained in a solution of 20  $\mu$ g of propidium iodide and 250  $\mu$ g of ribonuclease (RNase) A per milliliter. Flow cytometry analysis was performed on a Becton-Dickinson FACScan, and data from 80,000 cells per sample were analyzed with the CellFIT Cell Cycle Analysis software. A gate was set to select CD20-positive cells with FITC staining at least 20 times stronger than that in the negative untransfected cells. Other gates were selected for single cells within a normal size range. The propidium iodide signal was used as a measure for DNA content and hence cell cycle stage. The DNA histograms each contain data from 1000 to 5000 CD20-positive cells.
  23. Associated cyclins were detected in re-immunoprecipitation experiments. We transfected U2OS cells with the tagged wild-type or mutant kinases and labeled them with <sup>35</sup>S-methionine. The HA-tag immunoprecipitations were denatured and re-immunoprecipitated with different anticyclin monoclonal antibodies.
  24. The DNA histograms of cells transfected with plasmids expressing the wild-type kinases were indistinguishable from controls transfected with the CMV vector.
  25. Expression of the Cdk2-dn mutant resulted in a G<sub>1</sub> arrest in all cell lines tested, including U2OS and Saos-2 osteosarcoma cells, C33A cervical carcinoma cells, T98G glioblastoma cells, and 293 human adenovirus-transformed kidney cells. The Cdc2-dn effect was most prominent in U2OS cells, and similar effects were seen in Saos-2 and T98G cells. However, the cell cycle distribution of C33A cells was not affected by this mutant. This latter result stresses that absence of a dominant-negative phenotype in this assay does not exclude a cell cycle function for the wild-type kinase in normal cells. Transformed cells may be resistant to dominant-negative inhibition, for example, as a result of overexpression of cyclins, activating kinase mutations or loss of growth-control pathways.
  26. P. W. Hinds *et al.*, *Cell* 70, 993 (1992).
  27. S. van den Heuvel and E. Harlow, unpublished data.
  28. We transfected Saos-2 cells with different amounts of the plasmids encoding HA-tagged mutant Cdk2 or Cdk3 and analyzed them by flow cytometry. Lysates from cells that showed equally increased G<sub>1</sub> populations were examined to quantitate the Cdk2-dn and Cdk3-dn protein levels. A serial dilution of the lysates (containing 0.2,

- 1, 5, or 25  $\mu$ g of protein) was separated by SDS-PAGE, immunoblotted, and probed with the 12CA5 antibody. The same G<sub>1</sub> increase appeared to be obtained with an amount of Cdk3-dn protein 1/10 to 1/20 of that of Cdk2-dn protein.
29. M. Meyerson and S. van den Heuvel, unpublished data.
30. J. Lew, R. J. Winkfein, H. K. Paudel, J. H. Wang, *J. Biol. Chem.* 267, 25922 (1992); L.-H. Tsai, T. Takahashi, V. S. Caviness Jr., E. Harlow, *Development*, in press.
31. S. J. Baker, S. Markowitz, E. R. Fearon, J. K. V. Willson, B. Vogelstein, *Science* 249, 912 (1990).
32. F. L. Graham and A. J. Van der Eb, *Virology* 52, 456 (1973); F. M. Ausubel *et al.*, Eds., *Current Protocols in Molecular Biology* (Wiley, New York, 1988), vol. 1.

33. L. Zhu *et al.*, *Genes Dev.* 7, 1111 (1993).
34. We thank D. Dombkowski for his help with the flow cytometry analysis, P. Hinds for the cyclin expression plasmids, I. Stamenkovic for the CD20 cDNA, G. Enders for the HA-tagged PCTAIRE-1 clone, and M. Vidal for help with the yeast experiments. M. Meyerson, L.-H. Tsai, E. Lees, K. Helin, J. Lees, and A. Fattaey are acknowledged for their careful reading of the manuscript. S.v.d.H. is a recipient of fellowships from the Netherlands Organization for Scientific Research (NWO) and the Helen Hay Whitney Foundation. E.H. is an American Cancer Society Research Professor and is supported by grants from the National Institutes of Health.

27 July 1993; accepted 20 October 1993

## Receptive Field Reorganization in Dorsal Column Nuclei During Temporary Denervation

Michael J. Pettit and Harris D. Schwark\*

Altered sensory input can result in the reorganization of somatosensory maps in the cerebral cortex and thalamus, but the extent to which reorganization occurs at lower levels of the somatosensory system is unknown. In cat dorsal column nuclei (DCN), the injection of local anesthetic into the receptive fields of DCN neurons resulted in the emergence of a new receptive field in all 13 neurons studied. New receptive fields emerged rapidly (within minutes), sometimes accompanied by changes in adaptation rates and stimulus selectivity, suggesting that the new fields arose from the unmasking of previously ineffective inputs. Receptive field reorganization was not imposed by descending cortical inputs to the DCN, because comparable results were obtained in 10 additional cells when the somatosensory and motor cortex were removed before recording. These results suggest that mechanisms underlying somatotopic reorganization exist at the earliest stages of somatosensory processing. Such mechanisms may participate in adaptive responses of the nervous system to injury or continuously changing sensory stimulation.

Sensory maps in the cerebral cortex are maintained through dynamic processes. Modification of peripheral inputs to the central nervous system results in reorganization of cortical somatosensory maps in a number of species (1) including humans (2). The identification of the mechanisms that are involved in map reorganization has clinical implications for the treatment of peripheral nerve injury and phantom limb pain.

A critical issue that must be resolved before the mechanisms of reorganization can be uncovered is the extent to which reorganization at subcortical levels contributes to changes previously described in the cortex. Mapping studies suggest that peripheral nerve transection can result in map reorganization in the primate ventral posterior thalamic nucleus (3). Such reorganization has not been found in DCN or trigeminal nuclei (4), although it is difficult to detect reorganization in subcortical maps, which are three-dimensional and can exhibit large somatotopic shifts over relatively

small distances. An alternative approach, which we have used in the present study, is to map a single neuron's receptive field, inject local anesthetic into the field to silence input from the receptive field temporarily, and then test for the appearance of a new receptive field. In thalamus (5) and cortex (6) this approach has been used to demonstrate that new receptive fields can emerge within minutes after the injection of lidocaine. Such changes in cat DCN neurons have not been investigated, although cold block of the dorsal columns has been reported to result in the emergence of new receptive fields in a small proportion of nucleus gracilis neurons (7).

To study subcortical reorganization in the present experiments, we recorded from 13 DCN neurons in six adult cats (8). Subcutaneous lidocaine injections into the original receptive field resulted in the rapid emergence of a new receptive field in every neuron tested (Table 1 and Fig. 1, A and B). However, the possibility remained that the primary site of reorganization was the cerebral cortex, and that subcortical reorganization was imposed by descending cortical inputs to the DCN. To test this possibility, we recorded from 10 neurons in four additional cats after the re-

Department of Biological Sciences, University of North Texas, Denton, TX 76203.

\*To whom correspondence should be addressed.